ELSEVIER

Ultramicroscopy 89 (2001) 291–298

ultramicroscopy

www.elsevier.com/locate/ultramic

Potential-induced resonant tunneling through a redox metalloprotein investigated by electrochemical scanning probe microscopy

Paolo Facci*, Dario Alliata, Salvatore Cannistraro

Istituto Nazionale per la Fisica della Materia, C/o Dipartimento di Scienze Ambientali, Università della Tuscia, Via San C. de Lellis, 01100 Viterbo, Italy

Received 14 February 2001; received in revised form 1 March 2001

Abstract

The redox metalloprotein azurin self-chemisorbed onto Au(1 1 1) substrates has been investigated by electrochemically controlled scanning tunneling (STM) and scanning force/lateral force microscopy (SFM/LFM) and cyclic voltammetry (CV) in aqueous solution. The combined use of STM and SFM/LFM under electrochemical control in the negative side of the azurin redox midpoint (+116 mV vs. SCE) has delivered unique information on the nature of the STM images. While in STM the bright spots, believed to be associated with azurin molecules, are visible only for potential values higher than −125 mV, the concurrent electrochemical SFM results show adsorbed proteins over the whole potential range investigated (from −225 to +75 mV). Stepping the potential back and forth (between −25 and −125 mV) in STM imaging, it has been possible to make bright spots appearing and disappearing repeatedly, indicating that STM image formation arises possibly through resonant tunneling via the redox levels of azurin. These results represent the first clear evidence of potential-dependent tunneling in proteins adsorbed onto a conductive substrate.

1. Introduction

The study of the electron transfer behavior of molecules and biomolecules immobilized onto metal electrodes represents an interesting and important task since it is intimately connected to the charming possibility of deeply understanding and tuning their functional properties [1]. Moreover, functional metalloproteins at the metal surface form the basic elements also for researches in different frontier fields such as biosensors [2,3] and biomolecular electronics [4]. Several surface techniques have been employed to study the molecular organization and the redox properties of metalloproteins immobilized onto metal surfaces [5]. Particularly, scanning probe microscopy (SPM) techniques operating under electrochemical control [6] allow to perform this investigation at the level of a single molecule, hence contributing also to the recent general effort toward the detection and identification of single molecules [7].

In the recent past different STM works on metalloproteins [8–10] and other redox molecules [11] adsorbed onto atomically flat metal surfaces have been carried out aiming at the investigation

*Corresponding author.
E-mail address: Pacci@unitus.it (P. Facci).

0304-3991/01/$ - see front matter
PII: S0304-3991(01)00093-6

of electron transfer through immobilized species. Various theoretical predictions [12] and data explanations [13] have been provided for accounting for the STM signal involving resonant tunneling (possibly assisted by nuclear relaxation) [14] or two-step processes such as reduction–oxidation [15]. Very few works, however, have taken advantage of the full control of this reaction by tuning the electrochemical potential (i.e. Fermi levels) of the two working electrodes (substrate and tip) with a bipotentiostat. Furthermore, to our knowledge, the resonant nature of the tunneling current through adsorbed redox centers has been exhaustively revealed only by Tao [11] in the case of a rather simple molecule such as Fe(III)-protoporphyrin.

In this work we face the problem of understanding the nature of the current recorded in STM imaging of the blue copper protein azurin by a combined STM and SFM/LFM investigation under electrochemical control.

Azurin [16] is an electron transfer metalloprotein (molecular mass 14 600) involved in respiratory phosphorylation of the bacterium *Pseudomonas aeruginosa*. Its redox active center contains a copper ion liganded to five aminoacid atoms according to a peculiar ligand-field symmetry which endows the center with unusual spectroscopic and electrochemical properties such as an intense electron absorption band at 628 nm (due to the S(Cys-σ)$\rightarrow$Cu charge transfer transition), a small hyperfine splitting in the electron paramagnetic spectrum [17] and an unusually large equilibrium potential ($+116$ mV vs. SCE) [18] in comparison to the Cu(II/I) aqua couple (-89 mV vs. SCE) [19]. Moreover, Azurin has been imaged by *in situ* STM exploiting its self-assembling capabilities onto gold via a surface disulfide bridge (Cys3–Cys26) [8,14] or via a single surface Cys residue inserted by protein engineering [20].

2. Experimental section

2.1. Chemicals

Azurin from *Pseudomonas aeruginosa* was purchased from Sigma and used without further purification after having checked that the ratio OD_{628}/OD_{280} (OD_λ = optical density measured at λ nm) was in accordance with literature values (0.53–0.58) [21]. Working solution was 10^{-4} M azurin in 50 mM NH_4Ac (Sigma) buffer, pH 4.6. The buffer was degased with N_2 flow prior to use. Milli-Q grade water (resistivity 18.2 MΩ cm) was used throughout all the experiments.

2.2. Substrates

Au(1 1 1) substrates were prepared by evaporating 150-nm-thick Au films onto freshly cleaved mica sheets. The sheets were first baked for 2 h at 450°C and 10^{-7} mbar; Au evaporation was performed at 0.1 nm/s deposition rate. After evaporation the films were let annealing for 30 min at 550°C and 10^{-5} mbar. After cooling down to room temperature, a moderate flame annealing was necessary to get large re-crystallized Au(1 1 1) terraces.

2.3. Probes

STM tips were made from PtIr (80 : 20) by electrochemical etching of a 0.25 mm wire in a melt of $NaNO_3$ and NaOH [22]. Tips were then insulated with molten Apiezon wax. Only tips displaying leakage levels below 10 pA were used for imaging.

For SFM/LFM, SiO_2 Ultralevers (Thermomicroscopes Co.) with elastic constant of 0.06 N/m and apex curvature radius of 10 nm were used.

2.4. Sample preparation

Freshly prepared Au(111) substrates were incubated in 10^{-4} M azurin for 20–40 min (3 days at 4°C for CV) and then rinsed in abundant NH_4Ac buffer directly in the measuring cell, leaving always an aqueous layer on the top of the substrate to prevent protein exposure to water surface tension. After several rinsing cycles the measuring cell was filled with the same buffer and immediately installed in the microscope for imaging (or for CV measurements). In case of SFM/LFM measurements, incubation time was kept at 20 min in

order to have a rather low surface density which allows for a more defined single protein resolution.

2.5. Cyclic voltammetry

Samples, incubated directly in the SPM measuring cell, were measured with a Picostat (Molecular Imaging Co.) potentiostat at scanning rates in the range 0.01–0.005 V/s in the potential window (−0.25 to +0.3 V). Other details on the electrochemical measurements are reported in the following section.

2.6. In situ SPM

A Picoscan system (Molecular Imaging Co.) equipped with a Picostat (Molecular Imaging Co.) bipotentiostat was used to perform in situ SPM investigation. The measuring cell consisted of a Teflon™ ring pressed over the Au(1 1 1) substrate operating as working electrode. A 0.5 mm Pt wire was used as counter electrode and a 0.5 mm Ag wire as quasi-reference electrode (AgQref). The AgQref potential was measured vs SCE before and after each experiment. In what follows the potentials will be always referred to SCE. In order to minimize buffer evaporation, the cell was mounted into a sealed Pirex™ chamber. Images were acquired at room temperature under electrochemical control in the potential range −225 to +75 mV at steady state current conditions.

A 10 μm scanner with a final preamplifier sensitivity of 1 nA/V and a 6 μm scanner were used for STM and SFM/LFM measurements, respectively.

STM images were acquired in constant current mode with a typical tunneling current of 2 nA, bias voltage of 400 mV (tip positive), and scan rate of 4 Hz.

The typical tip–sample interaction force for SFM/LFM was 1 nN at 2–4 Hz scan rate.

3. Results and discussion

It is now well accepted [8,9,13,14] that azurin can be studied by in situ STM under full electrochemical control provided by a bipotentiostat which enables to control separately the electrochemical potential of the two working electrodes involved in the measurement, i.e. substrate and tip. Recently, the redox activity of gold immobilized azurin has been reported [18] and the presence of the copper has been claimed as a result of X-ray photoelectron spectroscopy [8] Fig. 1 reports an STM image acquired at a substrate potential of −25 mV. Bright spots 3–4 nm in lateral size (full width at half maximum) appear on the flat surface of Au(1 1 1) terraces. These figures are in general agreement with the crystallographic size of azurin [23]. The surface density of the spots can be largely tuned by varying incubation time, protein concentration, and temperature from few molecules per square micrometer up to a rather dense monolayer.

High surface densities, corresponding to about 90% coverage, as estimated by microgravimetric measurements (data not shown), have been used to record CV curves of the adsorbed azurin molecules. Fig. 2 shows the corresponding results. From this data, a redox midpoint of +120 mV, consistent with the solution data available from the literature [18] for azurin, results. The marked depression of the anodic peak, along with the rather large peak separation (160 mV) seems to point out the involvement of a mechanism of slow electron transfer, that has been already reported in electron transfer studies of this protein [14]. These

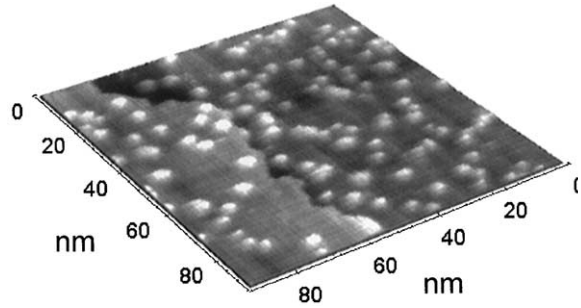

Fig. 1. Three-dimensional image showing azurin-adsorbed Au(1 1 1) recorded in 50 mM NH_4Ac (pH 4.6) by in situ electrochemical STM in the constant-current mode. The image was taken at a scan rate of 4 Hz with a substrate potential of −25 mV, a tunneling current of 2 nA, and a bias voltage of 400 mV (tip positive). Scan area, $92.7 \times 92.7\ nm^2$. Vertical range, 1.7 nm.

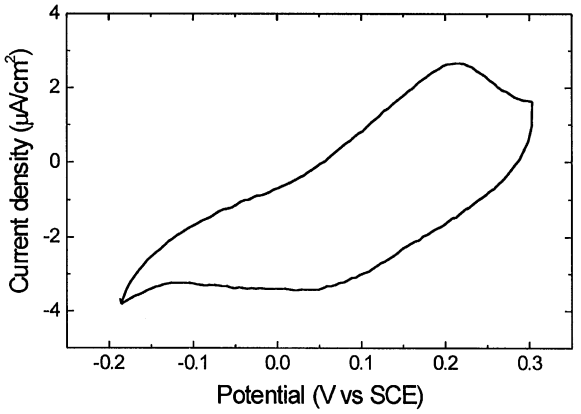

Fig. 2. Cyclic voltammogram of azurin coated Au(1 1 1) electrode in NH_4Ac 50 mM, pH 4.6, $T = 25°C$. Redox midpoint +120 mV, peak separation 160 mV, sweeping rate 5 mV/s.

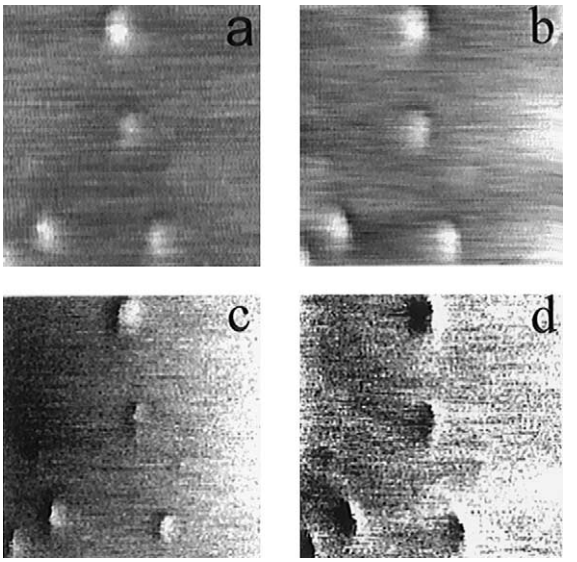

Fig. 3. Topography (a, b) and friction (c, d) images of azurin-adsorbed Au(1 1 1) in 50 mM NH_4Ac (pH 4.6) measured by in situ SFM/LFM at −225 mV at a scan rate of 4 Hz, in contact mode. Scan area, $150 \times 150\,nm^2$; vertical range, 1.1 nm (a, b). Images (a, c) forward scan, (b, d) backward scan.

data thus indicate the presence of redox-active azurin molecules on the surface of the gold electrode.

An intermediate–low density is mostly suited for investigating the behavior of the sample at the level of a single molecule by a combined STM-SFM/LFM approach. In fact, a joint SFM/LFM investigation can help in assessing the nature of the spots seen by STM. Fig. 3 shows a constant force (upper set) and the corresponding friction (lower set) images (a, c forward; b, d backward scan). Also in this case the sample appears as spots on a flat surface whose lateral size is however overestimated (10–20 nm) due to tip–adsorbate convolution [24]. The sample height is also different from the crystallographic one due to the tip pressure and results to be about 1 nm. However, while distinct spots are visible in both the scanning directions in constant force mode, the reversal of the contrast in the corresponding lateral force images clearly outlines the different friction sensed by the scanning tip over the spots and the surrounding flat areas. This is a sort of strong "spectroscopic" hint toward assessing the nature of the features which are visible by this microscopy technique [25].

In order to provide a deeper insight into the mechanism ruling the appearance of the features seen by us and previously reported in the literature [8,9,14] when imaging azurin by in situ electrochemical STM, we have carried out a parallel STM–SFM experiment under electrochemical control, i.e. by imaging the samples as a function of the substrate potential. Fig. 4 shows a sequence of SFM (upper set) and STM (lower set) images acquired at −225, −125, −25, and +75 mV, i.e. on the negative side of the redox midpoint of azurin (measured from cyclic voltammetry) and in a potential range where the Au(1 1 1) surface structure is still unaffected by the buffer ion adsorption [26]. Note that in case of SFM, the protein surface density has been kept to a minimum in order to limit the effect of tip–sample convolution.

While the SFM images show spots corresponding to azurin adsorbates in the whole set of potential values, albeit a certain drift and the mechanical removal of some proteins due to recurrent scans, the STM data look completely different. In fact the typical bright spots which are repeatedly seen when tuning the substrate potential to the proper region, now appear to be strongly potential-dependent since they switch on only between −125 and −25 mV.

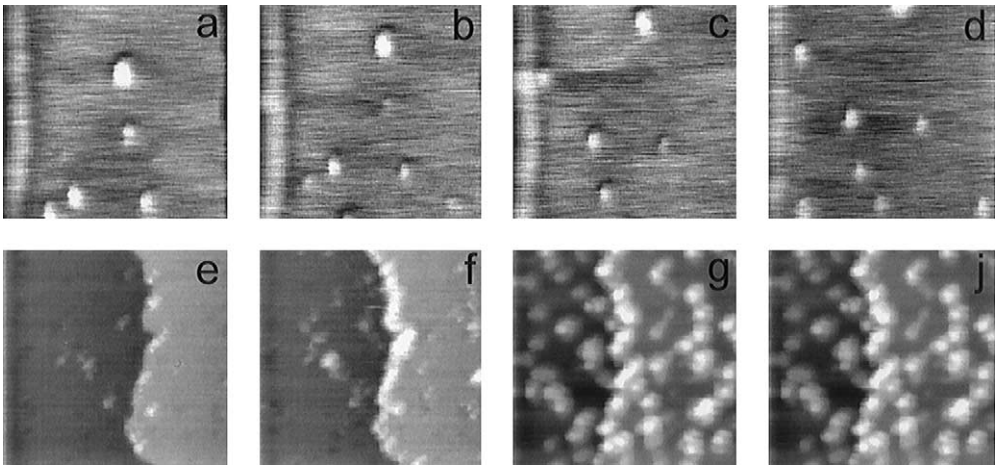

Fig. 4. Upper set, in situ SFM images recorded at −225 mV (a), −125 mV (b), −25 × mV (c) and +75 mV (d) in contact mode. Scan area, $200 \times 200\,nm^2$. Vertical range, 1 nm. Scan rate, 4 Hz. Lower set, in situ STM images recorded at −225 mV (e), −125 mV (f), −25 mV (g) and +75 mV (j) (tunneling current, 2 nA; bias, 400 mV tip positive). Scan area, $70 \times 70\,nm^2$; vertical range, 2 nm. Scan rate, 4 Hz.

Therefore, while the topographic SFM images are not affected by changes in the electrochemical potential of the substrate, STM images appear to be unambiguously dependent on tuning its value to that of the azurin redox midpoint.

Such a kind of behavior is consistent with a resonant nature of the current measured in STM experiments in gold-adsorbed azurin samples. Tunneling appears to take place via the protein redox level once the substrate potential is properly tuned to it.

The limitations imposed by the particular experimental system do not allow to follow the resonance profile also for more positive substrate values, overcoming the equilibrium potential of azurin and eventually monitoring the corresponding potential de-tuning. In fact, likely due to buffer ion adsorption on Au surface and the consequent lift of the reconstruction, more positive potential values do not allow for molecular resolution; rather, they result in an adlayer formation which stacks up as the potential is increased. The only consideration that can be done is that, since the redox midpoint of the immobilized protein and that of the solution counterpart do not differ drastically, it is possible to figure out a width of the resonance profile of about 300 mV which corresponds to the value observed also in the experiment of Tao in case of Fe(III)-protoporphyrins IX [11] and similarly appears to be underestimated with respect to the predictions of Marcus' electron transfer theory [27] (see note). The impossibility of measuring experimentally the reduction of azurin in this experimental setup prevents a more precise assessment of this width.

Interestingly, we note that, as far as the potential remains in the aforementioned range, it is possible to step back and forth its value and switch accordingly on and off the visible spots. Fig. 5 reports such an example, in which the potential is stepped by 100 mV to a more negative value (from −25 to −125 mV) and then is tuned back to the original value.

The molecular features, clearly visible in the first image (a), disappear in the second (b) for reappearing only once the potential is reestablished (c). It is also remarkable that in the image at −125 mV some darker zones appear in correspondence to the brighter spots in the other two images. These effective depressions can be interpreted in the proposed framework as a consequence of the STM feedback response to the local variation in the sample conductivity, suggesting once more that when the substrate

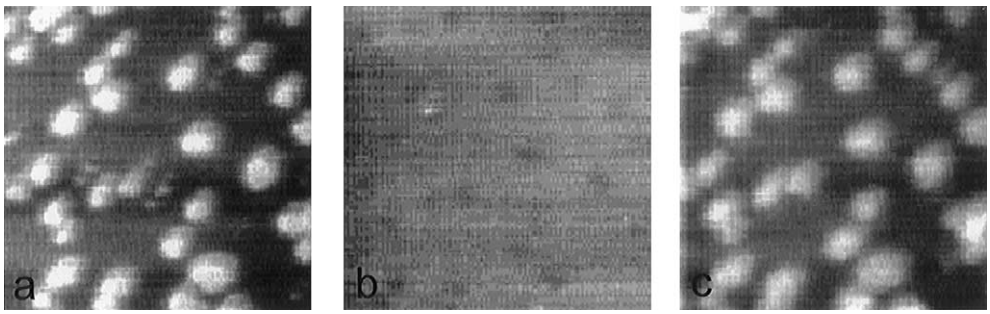

Fig. 5. Sequence of in situ STM images of azurin-adsorbed Au(1 1 1) in 50 mM NH_4Ac (pH 4.6) obtained at −25 mV (a), −125 mV (b) and −25 mV (c). Bias voltage, 400 mV (tip positive); tunneling current, 2 nA. Scan area, $45 \times 45\,nm^2$; vertical range, 1 nm. Scan rate 4 Hz.

potential is not tuned to the redox midpoint of azurin, the protein itself cannot elicit a current flow through it; rather, it behaves as an insulating barrier. This evidence is somehow confirmed also by the occurrence of a sort of blurring in Fig. 5c which could be consistently due to the interaction of the tip apex with the protein globule when scanning the surface in de-tuned conditions. However, several imaging cycles can be performed without a drastic loss of resolution.

In Fig. 6 we report the energy diagram (vs. SCE Fermi level E_F^{SCE}) relative to the measurements shown in Fig. 5. In fact, electrochemical potentials and Fermi levels are related by the Fermi level of the standard hydrogen electrode (−4.6 eV) [28] and hence by that of SCE. Particularly, Fig. 6a corresponds to the images 5a and 5c, i.e. to those acquired when the substrate potential was tuned to the states of the redox center (broadened by $\cong$300 meV), while Fig. 6b represents the situation observed in Fig. 5b. In the first case, tunneling takes place from the substrate to the tip (since tip is positive) via the redox states af azurin. In the second, since the substrate potential is not aligned to any molecular state, no resonance is elicited and consequently the bright spots disappear.

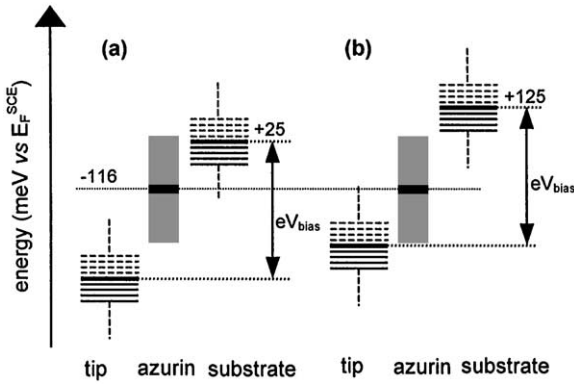

Fig. 6. Energy diagram of the experimental system in resonant (a) and non-resonant (b) conditions expressed in terms of SCE Fermi level (E_F^{SCE}); note the reversal of the sign in the energy values with respect to the corresponding potential values. The tip and substrate occupied (solid lines) and unoccupied (dashed lines) electronic states are separated by eV_{bias}, and rigidly shifted with respect to E_F^{SCE} by an energy amount provided by the substrate potential. The thick lines at tip and substrate represent their Fermi levels. The gray band, centered at the azurin equilibrium potential represents the molecule redox states (width $\cong$300 meV). If the substrate potential is tuned to the molecule redox states (a), as in the case of Fig. 5a and c, tunneling through these states is possible giving rise to bright spots in STM images; if, on the contrary, the potential does not match these states (b), resonant tunneling is inhibited, Fig. 5b.

These data demonstrate that the origin of the bright spots visible when performing in situ STM of gold-adsorbed azurin under electrochemical control is strictly potential-dependent. Unfortunately, experimental uncertainties preclude at this stage the possibility of assessing the exact physical mechanism (whether 1 step resonant tunneling or two-step single molecule electrochemistry [15]) governing the observed phenomenon. To our knowledge, however, this is the first time that such a behavior has been unambiguously observed on a biomolecule. Such results, moreover, provide the basic ground for the future exploitation of protein redox properties in gateable molecular devices.

4. Concluding remarks

The concurrent in situ STM–SFM/LFM analysis of azurin self-chemisorbed on Au(1 1 1) substrates carried out in this work under full potentiostatic control allows to draw a number of conclusions.

Our STM data confirm the possibility, already outlined in recent works, of imaging azurin under electrochemical control.

CV data indicate the presence of redox active azurin immobilized on the gold substrate.

The nature of the features visible in SFM experiments has been assessed by a combined SFM/LFM investigation outlining the different physical–chemical nature of the adsorbates with respect to the surrounding zones.

By investigating the samples as a function of the electrochemical potential of the substrate in a combined STM/SFM experiment, the resonant nature of the current emerging from the protein appears as a plausible mechanism for tunneling (even if a two-step mechanism cannot be excluded at this stage). This current arises only when the substrate potential is properly tuned to the azurin redox states, whose width appears to be about 300 meV.

The data show also the reversibility of the tuning/de-tuning process as the substrate potential is stepped back and forth around the onset of the resonance.

This experiment represents the first clear evidence of potential-elicited tunneling through redox adsorbates of biological origin, possibly resonant in nature.

Further studies will be devoted to investigate finely the shape of the resonance profile, possibly also as a function of different solvents in order to try to figure out the role of solvent reorganization energy in the broadening of azurin redox states. Another important issue will be that of assessing the role of the particular metal ion at the active site in determining the electrochemical properties of the features observed by in situ STM.

Acknowledgements

Financial support from the National Institute for the Physics of Matter (INFM) is gratefully acknowledged. The authors are grateful to Laura Andolfi for her help in CV measurements.

Note. According to the Marcus' theory of electron transfer, the effect of solvent modes, which are considered in the framework of a continuum dielectric model, is that of inducing a broadening of the redox center states given by $w = 4(\lambda_{out} kT \ln 2)^{1/2}$, where k is the Boltzmann constant, T the absolute temperature and λ_{out} (typically 1 eV) is the solvent reorganization energy. The measured width could reflect the location of the redox center in azurin, buried inside the protein globule and hence not easily accessible to water molecules.

References

[1] J. Brash, L. Horbertt (Eds.), Proteins at Interfaces II, ACS Symposium Series, Vol. 602, American Chemical Society, Washington, DC, 1995.
[2] A.P.F. Turner, I. Karube, G. Wilson, (Eds.), Biosensors: Fundamentals and Applications, Oxford University Press, London, 1989.
[3] I. Willner, E. Katz, B. Willner, R. Blonder, V. Heleg-Shabtai, A.F. Buckman, Biosens. Bioelectron. 12 (1997) 337.
[4] M. Alper, H. Bayley, D. Kaplan, M. Navia (Eds.), Biomolecular Materials by Design, Symposium Held November 29–December 3, 1993, Boston, MA, USA (Materials Research Society Symposium, V), Material Research Society, 1994.
[5] M. Lösche, Curr. Opin. Solid State Mater. Sci. 2 (1997) 546.
[6] R. Wiesendanger, H.-J. Güntherodt (Eds.), Scanning Tunneling Microscopy II, Springer, Berlin, Heidelberg, 1995.
[7] J. Gaudioso, H.J. Lee, W.J. Ho, Am. Chem. Soc. 121 (1999) 8479.
[8] Q. Chi, J. Zhang, J.U. Nielsen, E.P. Friis, I. Chorkendorff, G.W. Canters, J.E.T. Andersen, J. Ulstrup, J. Am. Chem. Soc. 122 (2000) 4047 and references therein.
[9] E.P. Friis, J.E.T. Andersen, L.L. Madsen, P. Møller, R.J. Nichols, K.G. Olesen, J. Ulstrup, Electrochim. Acta 43 (1998) 2889.
[10] J.E.T. Andersen, K.G. Olesen, A.I. Danilov, C.E. Foverskov, P. Møller, J. Ulstrup, Bioelectrochem. Bioenerg. 44 (1997) 57.
[11] N.J. Tao, Phys. Rev. Lett. 76 (1996) 4066.
[12] W. Schmickler, Surf. Sci. 295 (1993) 43–56.
[13] J.E.T. Andersen, A.A. Kornyshev, A.M. Kuznetsov, L.L. Madsen, P. Møller, J. Ulstrup, Electrochim. Acta 42 (1997) 819.

[14] E.P. Friis, J.E.T. Andersen, Yu.I. Kharkats, A.M. Kuznetsov, R.J. Nichols, J.-D. Zhang, J. Ulstrup, Proc. Natl. Acad. Sci. USA 96 (1999) 1379.
[15] W. Han, E.N. Durantini, T.A. Moore, A.L. Moore, D. Gust, P. Rez, G. Leatherman, G.R. Seely, N. Tao, S.M. Lindsay, J. Phys. Chem. B 101 (1996) 10719.
[16] E.T. Adman, in: P.M. Harrison (Ed.), Topics in Molecular and Structural Biology: Metalloporteins, Chemie Verlag, Weinheim, 1985.
[17] A.S. Brill, Transition Metals in Biochemistry, Springer, Berlin, 1977.
[18] Q. Chi, J. Zhang, E.P. Friis, J.E.T. Andersen, J. Ulstrup, Electrochem. Commun. 1 (1999) 91.
[19] D.R. Lide (Ed.), CRC Handbook of Physics and Chemistry, 74th Edition, CRC Press, Boca Raton, 1993.
[20] J.J. Davis, C.M. Halliwell, H. Allen, O. Hill, G.W. Canters, M.C. van Amsterdam, M.P. Verbeet, New J. Chem. 10 (1998) 1119.
[21] B.G. Karlsson, T. Pascher, M. Nordling, R.H.A. Ardvisson, L.G. Lundberg, FEBS Lett. 246 (1989) 211.
[22] D. Alliata, Investigation of nanoscale intercalation into graphite and carbon materials by in situ scanning probe microscopy. Ph.D. Dissertation, University of Bern, 2000.
[23] H. Nar, A. Messerschmitd, R. Huber, M. van de Kamp, G.W. Canters, J. Mol. Biol. 221 (1991) 765.
[24] J. Vesenka, R. Miller, E. Henderson, Rev. Sci. Instrum. 65 (1994) 2249.
[25] E. Meyer, R. Overney, D. Brodbeck, L. Howald, R. Lüthi, J. Frommer, H.-J. Güntherodt, Phys. Rev. Lett. 69 (1992) 1777.
[26] D.M. Kolb, A.S. Dakkouri, N. Batina, in: A.A. Gewirth, H. Siegenthaler (Eds.), Nanoscale Probes of the Solid/Liquid Interface, NATO ASI Series, Vol. 288, Kluwer Academic Publishers, Dordrecht, 1995, pp. 263–284.
[27] R.A. Marcus, J. Chem. Phys. 24 (1956) 966.
[28] A.J. Bard, L.R. Faulker (Eds.), Electrochemical Methods, Wiley, New York, 1990, p. 634.